15

Order, chaos, and fractals

15.1 Hamilton systems

A **Hamilton system** of n **degrees of freedom** has n coordinates q_i and n momenta p_i whose time derivatives are partial derivatives

$$\dot{q}_i = \frac{\partial H}{\partial p_i} \qquad \text{and} \qquad \dot{p}_i = -\frac{\partial H}{\partial q_i} \tag{15.1}$$

of a hamiltonian H that is a function of the $2n$ q's and p's and possibly of the time t. The time derivative of any function $F(q, p)$ of the q's and p's is then

$$\begin{aligned} \frac{dF}{dt} &= \frac{\partial F}{\partial t} + \sum_{i=1}^{n} \frac{\partial F}{\partial q_i}\,\dot{q}_i + \frac{\partial F}{\partial p_i}\,\dot{p}_i = \frac{\partial F}{\partial t} + \sum_{i=1}^{n} \frac{\partial F}{\partial q_i}\,\frac{\partial H}{\partial p_i} - \frac{\partial F}{\partial p_i}\,\frac{\partial H}{\partial q_i} \\ &= \frac{\partial F}{\partial t} + [F, H] \end{aligned} \tag{15.2}$$

in which the last term is the **Poisson bracket** $[F, H]$.

A Hamilton system with n symmetries has n conserved quantities C_i. If time translation invariance is one of the symmetries, and if the hamiltonian H and the conserved quantities are time independent, then the system is **autonomous**, the hamiltonian is one of the conserved quantites, and its Poisson bracket with each of the conserved quantities vanishes $[C_i, H] = 0$. If the conserved quantities have vanishing Poisson brackets $[C_i, C_j] = 0$, then they are **in involution**. An autonomous Hamilton system of degree n that has n independent conserved quantities that are in involution is Liouville **integrable**. In principle, one can integrate Hamilton's equations (15.1) for such a system.

Example 15.1 (Harmonic oscillators)**.** The coordinates q_i and momenta p_i of a Hamilton system of n independent harmonic oscillators obey Hamilton's

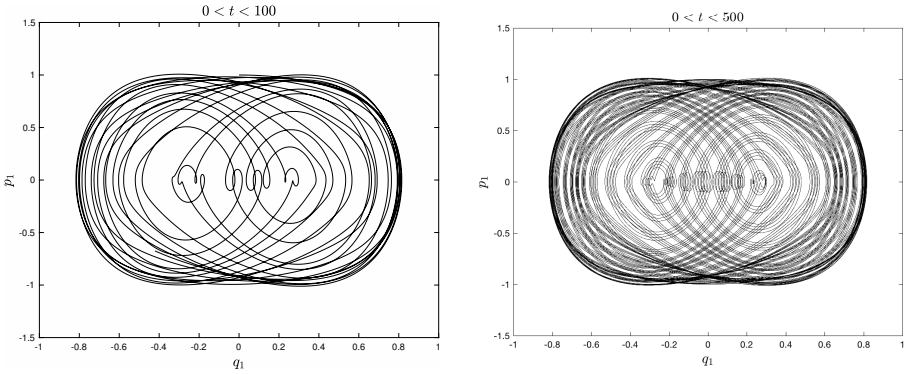

Figure 15.1 The $q_1(t), p_1(t)$ coordinates of a harmonic oscillator coupled to another harmonic oscillator by the hamiltonian (15.4) for $0 < t < 100$ (left) and $0 < t < 500$ (right). The initial conditions are $q_1 = q_2 = 0$ and $p_1 = p_2 = 1$, with $m = 1$, $\omega_2 = \omega_1/2 = 1/2$, and $\lambda = 1/2$.

equations

$$\dot{q}_i = \frac{p_i}{m_i} \qquad \text{and} \qquad \dot{p}_i = -\, m_i \omega_i^2\, q_i. \tag{15.3}$$

The energy $E_i = p_i^2/2m_i + m_i\omega_i q_i^2/2$ of each oscillator is conserved. The coordinates $q_i(t) = a_i \sin(\omega_i(t+\tau_i))$ and momenta $p_i = a_i m_i \omega_i \cos(\omega_i(t+\tau_i))$ run over the n-dimensional surface of an n-torus in a q, p phase space of $2n$ dimensions.

Few systems are integrable. Two coupled harmonic oscillators with

$$H = \frac{p_1^2 + p_2^2}{2m} + \frac{m(\omega_1^2 q_1^2 + \omega_2^2 q_2^2)}{2} + m\omega_1\omega_2(q_1 - q_2)^2 + \lambda\, q_1^2 q_2^2 \left(q_1^2 + q_2^2\right) \tag{15.4}$$

display complicated behavior as illustrated in Fig. 15.1 for equal masses but different frequencies.

□

Example 15.2 (The two-body problem)**.** Two interacting particles moving in empty 3-dimensional space are a system of 6 degrees of freedom with 7 conserved quantities—the energy $E_1 + E_2$, the momentum $\vec{p}_1 + \vec{p}_2$, and the angular momentum $\vec{r}_1 \times \vec{p}_1 + \vec{r}_2 \times \vec{p}_2$—which are in involution and independent. The system is integrable. Its motion is ordered, and if bounded, lies on the surface of a 6-torus. □

Hamilton systems are special: The $2n$ time derivatives $\dot{q}_i$ and $\dot{p}_i$ satisfy

(exercise 15.1) the identities

$$\frac{\partial \dot{q}_i}{\partial q_j} = -\frac{\partial \dot{p}_j}{\partial p_i}, \quad \frac{\partial \dot{q}_i}{\partial p_j} = \frac{\partial \dot{q}_j}{\partial p_i}, \quad \text{and} \quad \frac{\partial \dot{p}_i}{\partial q_j} = \frac{\partial \dot{p}_j}{\partial q_i}. \tag{15.5}$$

The integral

$$A = \oint \sum_{i=1}^{n} p_i \, dq_i \tag{15.6}$$

over a closed trajectory in phase space is a time-independent Poincaré invariant (example 12.9). Areas of phase space are constant in time (example 12.11) along Hamilton trajectories (15.1)

$$\frac{d}{dt}\left(\sum_i^n \begin{vmatrix} \delta p_i & \delta q_i \\ \Delta p_i & \Delta q_i \end{vmatrix} \right) = 0. \tag{15.7}$$

Although they are special, few Hamilton systems are integrable. Three interacting particles moving in empty space are a system of 9 degrees of freedom with only 7 independent conserved quantities. The three-body problem is not integrable.

15.2 Systems of ordinary differential equations

An autonomous system of n first-order ordinary differential equations

$$\begin{aligned} \dot{x}_1 &= F_1(x_1, x_2, \ldots, x_n) \\ \dot{x}_2 &= F_2(x_1, x_2, \ldots, x_n) \\ &\vdots \\ \dot{x}_n &= F_n(x_1, x_2, \ldots, x_n). \end{aligned} \tag{15.8}$$

is more general than it may seem at first sight. For a non-autonomous system of n equations with functions $F_i(x_1, \ldots, x_n, t)$ is equivalent to an autonomous system of $n+1$ equations with $t = x_{n+1}$ and $F_{n+1}(x_1, \ldots, x_{n+1}) = 1$. And a system of n higher-order ordinary differential equations is equivalent to an autonomous first-order system of more than n first-order ordinary differential equations.

Example 15.3 (Forced van der Pol oscillator)**.** The second-order, time-dependent differential equation $\ddot{y} + \mu(y^2 - 1)\dot{y} + y = a\sin(\omega t)$ describes a forced van der Pol oscillator. Setting $x_1 = \dot{y}$, $x_2 = y$, and $x_3 = t$, we may

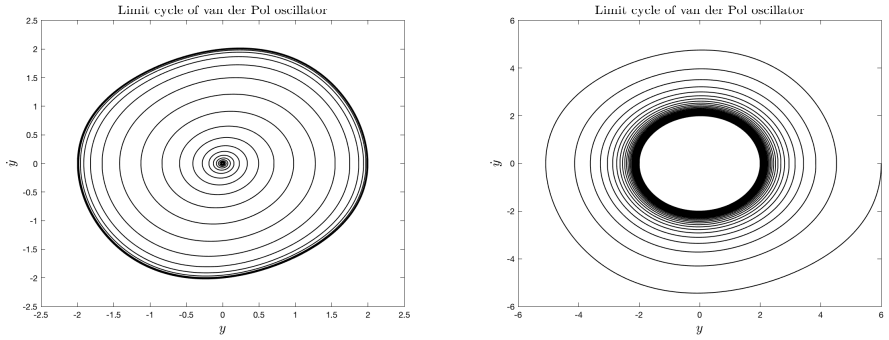

Figure 15.2 Trajectories of the unforced ($\omega = a = 0$) van der Pol oscillator (15.9) converge to their attractors which are limit cycles. The outward spiral starts from $y(0) = 0.01$ and $\dot{y}(0) = 0$ with $\mu = 1/8$ (left); the inward spiral starts from $y(0) = 6$ and $\dot{y}(0) = 0$ with $\mu = 1/64$ (right).

write it as the first-order autonomous system

$$\begin{aligned} \dot{x}_1 &= -x_2 - \mu(x_2^2 - 1)x_1 + a\sin(\omega x_3), \\ \dot{x}_2 &= x_1, \quad \text{and} \quad \dot{x}_3 = 1 \end{aligned} \tag{15.9}$$

which exhibits chaos for certain values of its parameters μ, a, and ω. The unforced oscillator ($\omega = a = 0$) has trajectories that converge to limit cycles as illustrated in Fig. 15.2. The outward spiral starts from $y(0) = 0.01$ and $\dot{y}(0) = 0$ with $\mu = 1/8$ (left); the inward spiral starts from $y(0) = 6$ and $\dot{y}(0) = 0$ with $\mu = 1/64$ (right).

□

15.3 Attractors

Hamilton systems evolve in ways that conserve their areas in phase space (15.7), but arbitrary autonomous systems evolve more generally. Phase-space areas of **dissipative** systems typically shrink. If they converge to a point or to a set of points, that point or set is an **attractor**. An attractor may be a point of dimension zero, a loop or **limit cycle** of dimension one, a surface of integral dimension, or a **fractal**—a set whose dimension is not an integer (section 15.6). A fractal attractor is a **strange attractor**.

Example 15.4 (Lorenz butterfly)**.** The Lorenz system is three first-order differential equations

$$\dot{x} = \sigma\,(y - x), \qquad \dot{y} = r\,x - y - x\,z, \qquad \dot{z} = x\,y - b\,z \tag{15.10}$$

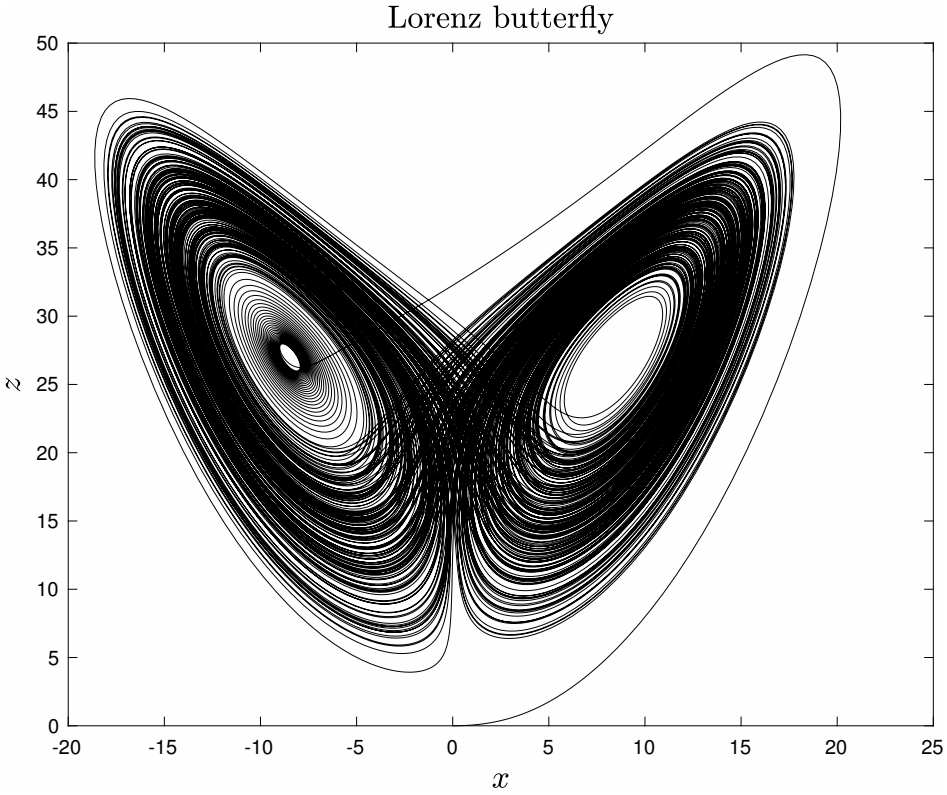

Figure 15.3 The trajectory of the Lorenz system (15.10) for $0 \leq t \leq 300$ approaches a strange attractor of dimension $D_{KY} = 2.06215$.

in which $\dot{y}$ and $\dot{z}$ have the nonlinear terms $-x\,z$ and $x\,y$, and the Prandtl number σ, the Rayleigh number r, and the parameter b are all positive. The Matlab code

```
x0 = [0 8 0]; tspan=[0,300];
[t,x]=ode45(@lorentz,tspan,x0); plot(x(:,1),x(:,3);
function xprime = lorentz(t,x); s = 10; b = 8/3; r =28;
xprime=[ - s*x(1) + s*x(2); r*x(1) - x(2) - x(1)*x(3); ...
- b*x(3) + x(1)*x(2) ]; end
```

generates the plot of $x = x(1)$ and $z = x(3)$ in Fig. 15.3 for initial conditions $x = z = 0$ and $y = 8$. □

Example 15.5 (Rössler system)**.** The solutions of the differential equations

$$\begin{aligned} \dot{x} &= -y - z \\ \dot{y} &= x + a\,y \\ \dot{z} &= b + z(x - c) \end{aligned} \tag{15.11}$$

with $a = b = 0.2$ and initial conditions $x(0) = y(0) = z(0) = 0$ display a simple limit cycle for $c = 2$, a period-two limit cycle for $c = 3$, a period-four limit cycle for $c = 4$, a period-eigth limit cycle for $c = 4.15$, and a strange attractor for $c = 5.7$ as shown in Fig. 15.4.

□

15.4 Chaos

Early in the last century, Henri Poincaré studied the three-body problem and found very complicated orbits. In this and many other systems, he found that after a transient period, classical motion assumes one of four forms:

1. periodic (a limit cycle)
2. steady or damped or stopped
3. quasi-periodic (more than one frequency)
4. chaotic

Chaos takes different forms in different dynamical systems, and no single definition of chaos fits all of them. Many are **extremely sensitive to initial conditions**. For instance, two trajectories $x(t) = (x_1(t), \ldots, x_n(t))$ and $x'(t) = (x'_1(t), \ldots, x'_n(t))$ of an autonomous system (15.8) may diverge from each other exponentially

$$\|\|x'(t) - x(t)\|\| = e^{\lambda t}\|\|x'(0) - x(0)\|\|. \tag{15.12}$$

in which λ is a **Lyapunov exponent**.

A first-order, autonomous dynamical system can be chaotic only it has at least $n = 3$ dimensions. The driven, damped pendulum (example 15.9), the Lorenz system (example 15.4), and the Rössler system (example 15.5) all have $n = 3$ and evolve chaotically for certain values of their parameters. Here are three more examples:

Example 15.6 (Duffing's equation)**.** If one attaches a thin piece of iron to the end of a rod that moves sinusoidally in the x direction at frequency ω

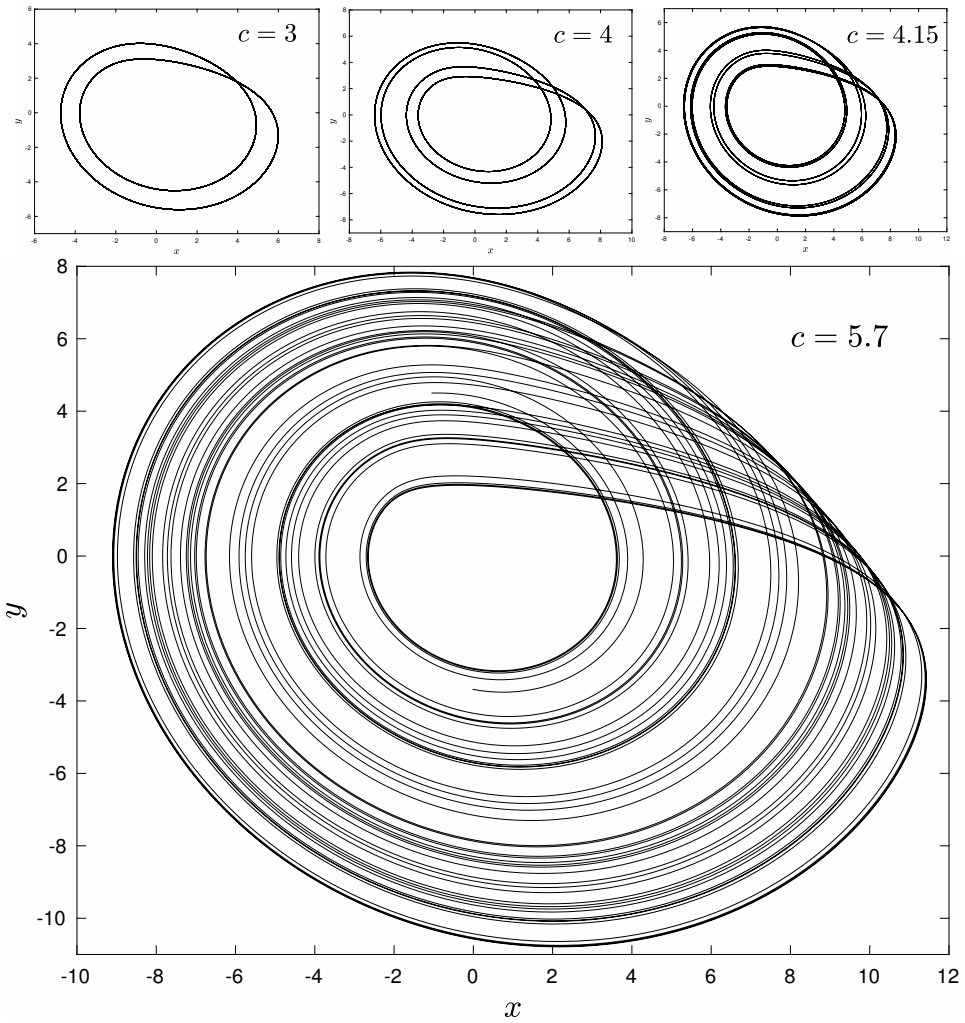

Figure 15.4 The last 10,000 points $(x(i), y(i))$ of the solution of the Rössler equations (15.11) trace the attractor for initial conditions $x(0) = y(0) = z(0) = 0$ and various values of the parameter c. For $c = 2$, the attractor is a simple loop (not shown); for $c = 3$, it is two loops loop; for $c = 4$, it is four loops; for $c = 4.15$, it is eight loops; and for $c = 5.7$, it is an infinite set of loops of dimension $D_{KY} = 2.0132$.

near two magnets, then the x coordinate is described by the forced Duffing equation

$$\ddot{x} + a\dot{x} + bx^3 + cx = g\sin(\omega t + \phi) \tag{15.13}$$

and varies chaotically for suitable values of a, b, c, g, ω, and ϕ. □

Example 15.7 (Dripping faucet)**.** Drops from a slowly dripping faucet tend to fall regularly at times t_n separated by a constant interval $\Delta t = t_{n+1} - t_n$. At a slightly higher flow rate, the drops fall separated by intervals that alternate in their durations Δt, ΔT, Δt, ΔT, Δt, ΔT in a **period-two** sequence. At some higher flow rates, no regularity is apparent. □

Example 15.8 (Rayleigh-Benard convection)**.** Consider a fluid in a gravitational field above a hot plate and below a cold one. If the difference ΔT is small enough, then steady convective cellular flow occurs. But if ΔT is above the chaotic threshold, the fluid boils chaotically. □

15.5 Maps

Successive crossings $x_j = (x_{1j}, \ldots, x_{nj})$ from one side to the other of a suitably oriented surface by an n-dimensional trajectory form a **Poincaré map**

$$x_{j+1} = M(x_j) \tag{15.14}$$

in a space of $n-1$ dimensions. Poincaré maps are invertible $x_j = M^{-1}(x_{j+1})$. An invertible map can be chaotic only if it has at least two dimensions so that it comes from a dynamical system that has at least three dimensions. A one-dimensional map that is not invertible can display chaos.

The Lyapunov exponent of a smooth one-dimensional map $x_{j+1} = f(x_j)$ is the limit

$$h(x_1) = \lim_{j \to \infty} \frac{1}{j} \left[\ln |f'(x_1)| + \ldots + \ln |f'(x_j)| \right]. \tag{15.15}$$

A bounded sequence that has a positive Lyapunov exponent and that does not converge to a periodic sequence is **chaotic** (Alligood et al., 1996, p. 110). Other aspects of chaos lead to other definitions.

Example 15.9 (Driven, damped pendulum)**.** The angle θ of a sinusoidally driven, damped pendulum obeys the differential equation

$$\ddot{\theta} + b\dot{\theta} + \sin\theta = F \cos t \tag{15.16}$$

which is second order and nonautonomous. We put it into autonomous form

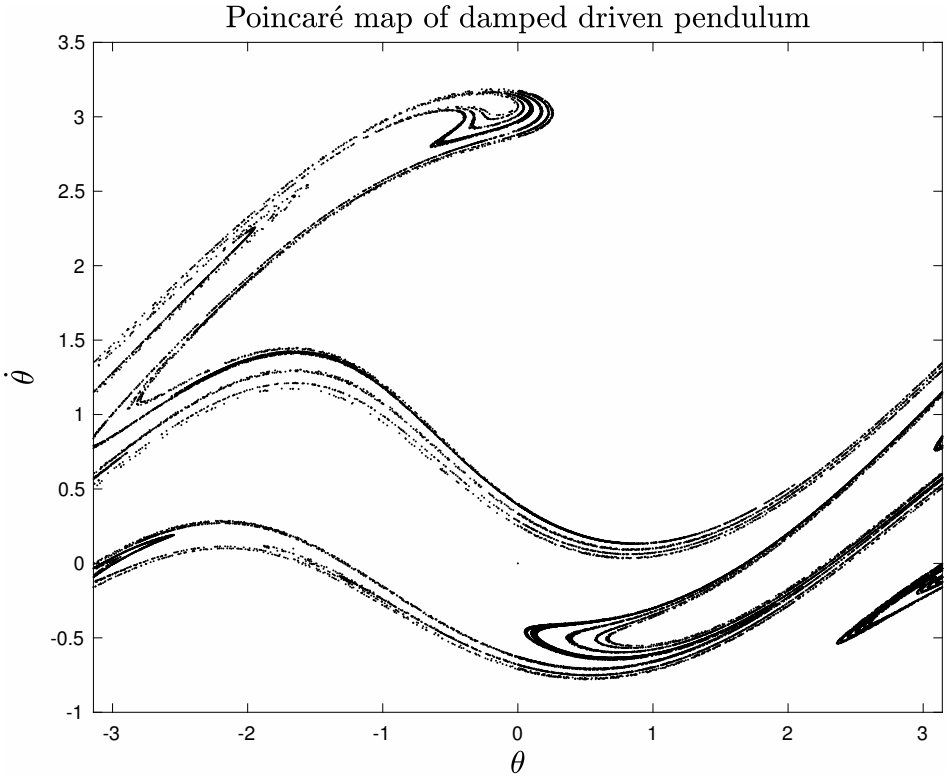

Figure 15.5 Poincaré map of the first million crossings of the surface $x_3 = 0 \pmod{2\pi}$ by the trajectory $(\theta(t), \dot{\theta}(t))$ of the damped driven pendulum (15.16) with $b = 0.22$ and $F = 2.7$. The points form a Cantor-set-like strange attractor of dimension $D_b \simeq 1.38$ (Grebogi et al., 1987). The initial conditions were $\theta(0) = \dot{\theta}(0) = 0$.

by defining $x_1 = \dot{\theta}$, $x_2 = \theta$, and $x_3 = t$. In these variables, the pendulum equation (15.16) is the first-order autonomous system

$$\begin{aligned} \dot{x}_1 &= F \cos x_3 - \sin x_2 - b\, x_1, \\ \dot{x}_2 &= x_1, \quad \text{and} \quad \dot{x}_3 = 1 \end{aligned} \tag{15.17}$$

with $n = 3$ dependent variables. Figure 15.5 displays a Poincaré map of the trajectory of the damped driven pendulum (15.16) with $b = 0.22$ and $F = 2.7$. This map is a strange attractor of dimension $D_b \simeq 1.38$ (Grebogi et al., 1987). The horizontal axis is the angle $\theta(2\pi j)$ modulo 2π [that is, $\text{sign}(\theta)\ \text{mod}(|\theta|,\, 2\pi)$] for $j = 0, 1, 2, \ldots, 10^6$ or the first million crossings of the surface $x_3 = 0 \bmod 2\pi$.

□

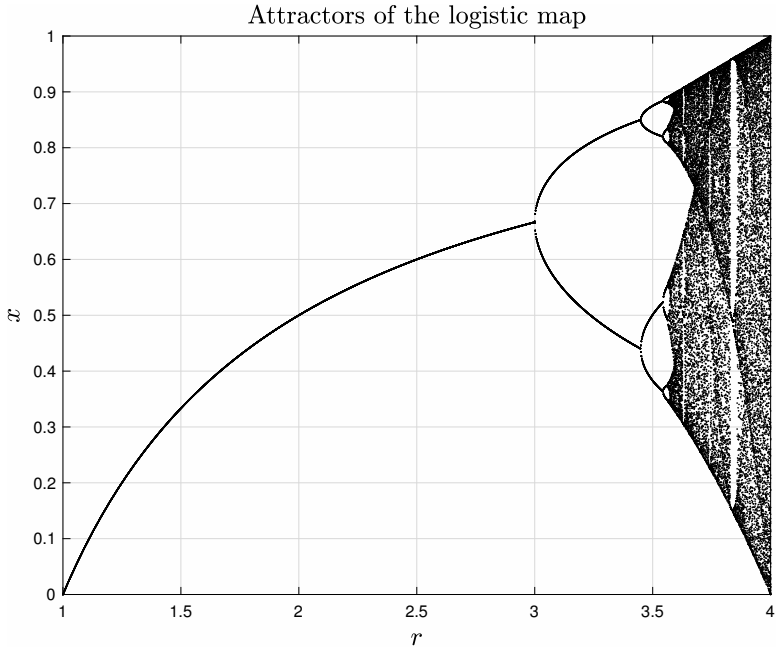

Figure 15.6 Points x_j of the logistic map (15.18) for $29990 \le n \le 30000$ and 10 random starting points $0 < x_0 < 1$ for $0.5 \le r \le 4$. From $r = 1$ to $r = 3$, the attractor rises from 0 to 2/3 where it splits into two attractors.

Example 15.10 (Logistic map)**.** For $0 < r < 4$, the one-dimensional **logistic map**

$$x_{j+1} = r\, x_j (1 - x_j) \tag{15.18}$$

describes a population with a limited food supply as does the differential equation (6.99). Because the quadratic equation for x_j in terms of x_{j+1} has two solutions, the logistic map is not invertible. For $0 < r < 1$, sequences of x_i's starting from any $0 < x_0 < 1$ converge to 0. This **attractor** begins to rise at $r = 1$ and reaches 2/3 at $r = 3$ where it bifurcates into two attractors as shown in Fig. 15.6. These attractors split again at $r_2 = 1 + \sqrt{6} \approx 3.4495$, and again at $r_3 \approx 3.54409$, and again at $r_4 \approx 3.5644$. By $r_\infty \approx 3.569946$, the attractors have split an infinite number of times. Chaos appears in increasingly striking forms as r exceeds r_∞. At $r = 3.8$, two sequences respectively starting from $x_0 = 0.2$ and $x_0' = 0.20001$ differ after 19 iterations by seeming random amounts: 0.218 at $n = 21$, 0.623 at $n = 23$, and 0.723 at $n = 74$. At $r = 4$, the logistic map (15.18) is totally chaotic and equivalent to the **tent map** $x_{j+1} = 1 - 2|x_j - 1|$. The **2x-modulo-1 map** $x_{j+1} = 2x_j \bmod 1$ is similarly chaotic.

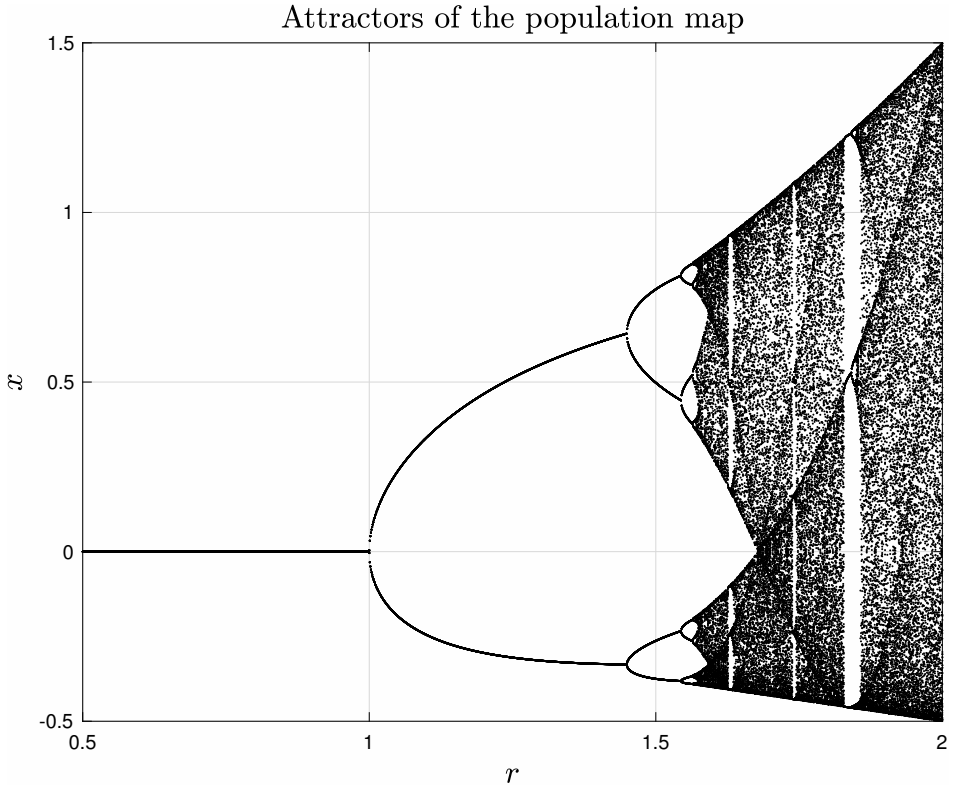

Figure 15.7 Points x_j of the population map (15.19) for $29990 \le n \le 30000$ and 10 random starting points $0 < x_0 < 1$ for $0.5 \le r \le 2$. For $0 \le r \le 1$, the attractor of the population map (15.19) is $x = 0$. The attractor splits at $r = 1$ into two attractors until $r_2 = \sqrt{2}$ where it splits into four. Slightly above $r_3 \approx 1.544$, the four attractors split into eight.

□

Example 15.11 (Population map)**.** For $0 < r < 2$, the map

$$x_{j+1} = r\, x_j(x_j - 1) \tag{15.19}$$

describes (for $x_j > 0$) a population whose rates of reproduction and death respectively are proportional to x_j^2 and x_j. For $r < 1$, sequences starting from any $0 < x_0 < 1$ approach the attractor $x = 0$ as shown in Fig. 15.7. That attractor splits at $r = 1$ into two attractors which become four at $r_2 = \sqrt{2}$. Somewhat above $r_3 \approx 1.544$, the four attractors split into eight. They split again at $r_4 \approx 1.565$. Chaos begins as r exceeds 1.57.

□

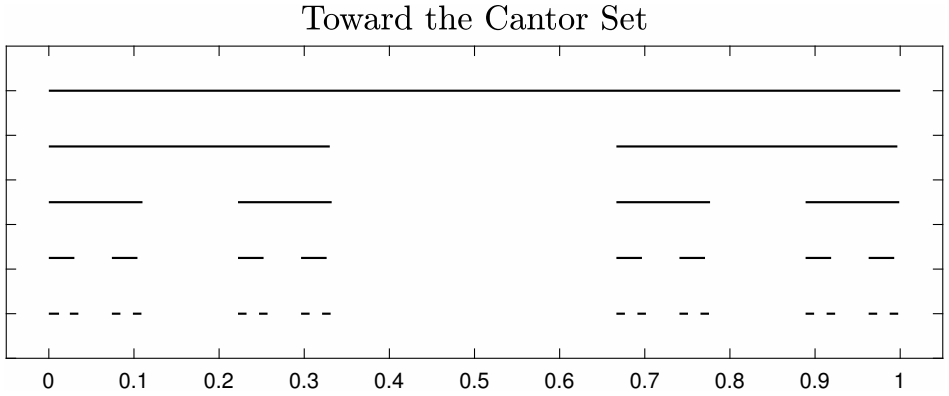

Figure 15.8 The first five approximations to the Cantor set.

Example 15.12 (The Bernoulli shift)**.** The simplest chaotic map is the **Bernoulli shift** in which the initial point x_0 is an arbitrary number between 0 and 1 with the binary-decimal expansion

$$x_0 = \sum_{k=1}^{\infty} 2^{-k} a_k = 0.a_1 a_2 a_3 a_4 \ldots \tag{15.20}$$

and successive points lack a_1, then a_2, and so forth:

$$x_1 = 0.a_2 a_3 a_4 a_5 \ldots, \quad x_2 = 0.a_3 a_4 a_5 a_6 \ldots, \quad x_3 = 0.a_4 a_5 a_6 a_7 \ldots. \tag{15.21}$$

Two unequal irrational numbers x_0 and x_0' no matter how close generate sequences that roam independently, irregularly, and ergotically over the interval $(0, 1)$. □

Example 15.13 (Hénon's map)**.** The two-dimensional map

$$\begin{aligned} x_{j+1} &= f(x_j) + B\, y_j \\ y_{j+1} &= x_j \end{aligned} \tag{15.22}$$

for $B \neq 0$ is invertible. If $f(x_j) = A - x_j^2$, it is **Hénon's map**, which for $A = 1.4$ and $B = 0.3$ is chaotic and converges to the attractor in Fig. 15.10. □

15.6 Fractals

A fractal set has a dimension that is not an integer. How can that be?

Felix Hausdorff and Abram Besicovitch have shown how to define the

dimension of a weird set of points. To compute their **box-counting** dimension of a set, we cover it with line segments, squares, cubes, or n-dimensional "boxes" of side ϵ. If we need $N(\epsilon)$ boxes, then the fractal dimension D is the limit as $\epsilon \to 0$

$$D_b = \lim_{\epsilon \to 0} \frac{\ln(N(\epsilon))}{\ln(1/\epsilon)}. \tag{15.23}$$

For instance, we can cover the interval $[a, b]$ with $N(\epsilon) = (b - a)/\epsilon$ line segments of length ϵ, so the dimension of the segment $[a, b]$ is

$$D_b = \lim_{\epsilon \to 0} \frac{\ln(N(\epsilon))}{\ln(1/\epsilon)} = \lim_{\epsilon \to 0} \frac{\ln((b-a)/\epsilon)}{\ln(1/\epsilon)} = 1 + \frac{\ln(b-a)}{\ln(1/\epsilon)} = 1 \tag{15.24}$$

as it should be.

Example 15.14 (Cantor set)**.** The Cantor set is defined by a limiting process in which the set at the nth stage consists of 2^n line segments each of length $1/3^n$. The first five approximations to the **Cantor set** are drawn in the figure (15.8). We can cover the nth approximation with $N(\epsilon) = 2^n$ line segments each of length $\epsilon_n = 1/3^n$, and so the fractal dimension is

$$D_b = \lim_{\epsilon \to 0} \frac{\ln(N(\epsilon))}{\ln(1/\epsilon)} = \lim_{n \to \infty} \frac{\ln(N(\epsilon_n))}{\ln(1/\epsilon_n)} = \lim_{n \to \infty} \frac{\ln(2^n)}{\ln(3^n)} = \frac{\ln 2}{\ln 3} = 0.6309297\ldots \tag{15.25}$$

which is not an integer or even a rational number. □

Example 15.15 (Koch Snowflake)**.** In 1904, the Swedish mathematician Helge von Koch described the Koch curve (or the Koch snowflake), whose construction is shown in Fig. 15.9. With each step, there are 4 times as many line segments, each one being 3 times smaller. The length L of the curve at step n is thus $L = (4/3)^n$ which grows without limit as $n \to \infty$. Its box dimension is

$$D_b = \lim_{n \to \infty} \frac{\ln(N(\epsilon_n))}{\ln(1/\epsilon_n)} = \lim_{n \to \infty} \frac{\ln(4^n)}{\ln(3^n)} = \frac{\ln 4}{\ln 3} = 1.2618595\ldots \tag{15.26}$$

□

Closely related to the box-counting dimension is the **self-similar dimension** D_s. To define it, we consider the number of self-similar structures of linear size x needed to cover the figure after n steps and take the limit

$$D_s = \lim_{x \to 0} \frac{\ln N(x)}{\ln 1/x}. \tag{15.27}$$

In the case of von Koch's curve, $x = 1/3^n$ and $N(x) = 4^n$. So the self-similar

The Koch Snowflake

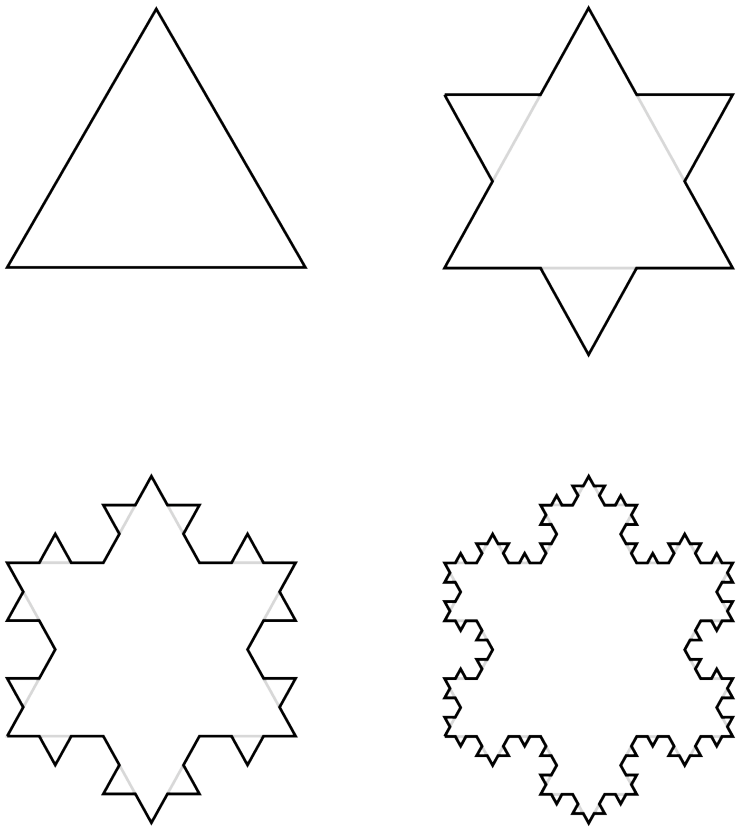

Figure 15.9 Curve of von Koch: Steps 0, 1, 2, and 3 of construction (adapted from Wikipedia).

dimension of von Koch's curve is

$$D_s = \lim_{x\to 0} \frac{\ln N(x)}{\ln 1/x} = \lim_{n\to\infty} \frac{\ln 4^n}{\ln 3^n} = \frac{n \ln 4}{n \ln 3} = \frac{\ln 4}{\ln 3} = 1.2618595\ldots \quad (15.28)$$

which is equal to its box dimension $D_{b,K}$ given by (15.26).

Other definitions of the dimension of a set, such as the correlation dimension D_2 (Grassberger and Procaccia, 1983) and the Kaplan-Yorke dimension D_{KY} (Kaplan and Yorke, 1979), can be easier to measure than the box-counting and self-similar dimensions.

Attractors of fractal dimension are **strange**. The Lorenz butterfly (exam-

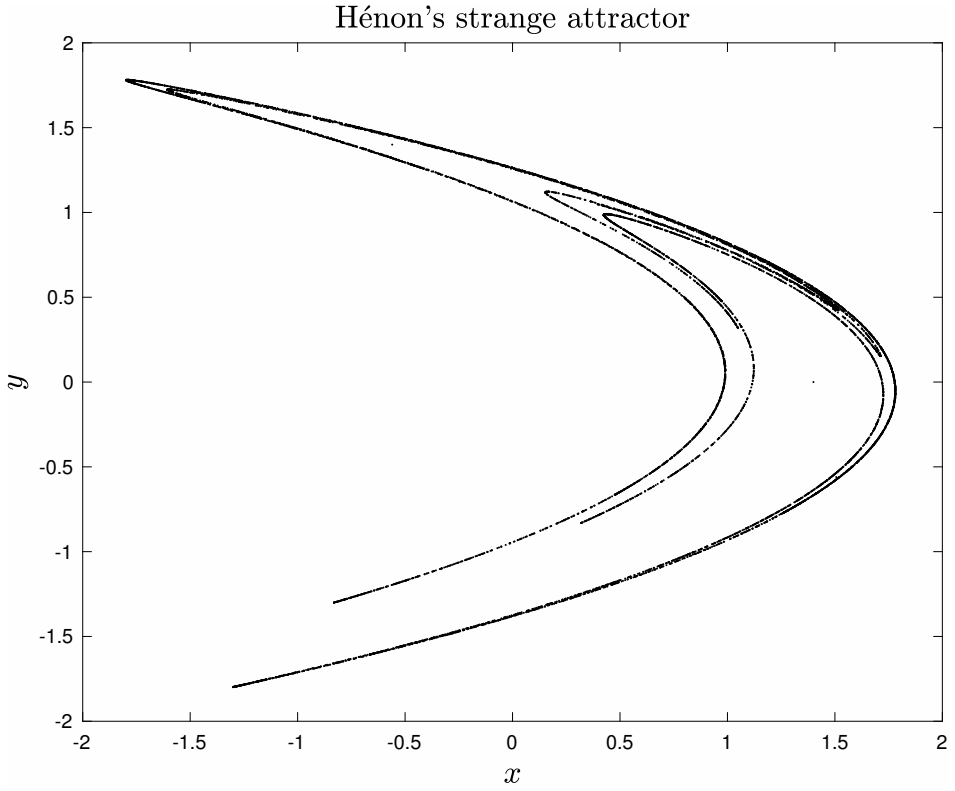

Figure 15.10 The first 10^4 points of the strange attractor of Hénon's map (15.13) with $A = 1.4$ and $B = 0.3$ and $(x_0, y_0) = (0, 0)$.

ple 15.4, Fig. 15.3) is a strange attractor of Kaplan-Yorke dimension $D_{KY} = 2.06215$, and the loops of the Rössler system for $c = 5.7$ (example 15.5, Fig. 15.4) form a strange attractor of dimension $D_{KY} = 2.0132$ (Sprott, 2003). The Poincaré map of the damped driven pendulum (15.16, Fig. 15.5 is a strange attractor of box-counting dimension $D_b \approx 1.38$ (Grebogi et al., 1987). Hénon's map (15.22, Fig. 15.10) with $A = 1.4$ and $B = 0.3$ is chaotic with a strange attractor of dimension $D_b = 1.261 \pm 0.003$ (Russell et al., 1980). Chaotic systems often have strange attractors; but chaotic systems can have nonfractal attractors, and nonchaotic systems can have strange attractors.

Further Reading

The books *Nonlinear Dynamics and Chaos: With Applications to Physics, Biology, Chemistry, and Engineering* (Strogatz, 2014), *CHAOS: An Intro-*

duction to Dynamical Systems (Alligood et al., 1996), and *Chaos and Time-Series Analysis* (Sprott, 2003) are superb.

Exercises

15.1 Use Hamilton's equations to derive the special relations (15.5) that the time derivatives $\dot{q}_i$ and $\dot{p}_i$ satisfy.

15.2 A period-one sequence of a map $x_{i+1} = f(x_i)$ is a point p for which $p = f(p)$. Find the period-one sequences of $x_{i+1} = rx_i(1 - x_i/K)$.

15.3 A period-two sequence of a map $x_{i+1} = f(x_i)$ is two different points p and q for which $q = f(p)$ and $p = f(q)$. Estimate the period-two sequences of the logistic map $f(x) = ax(1 - x)$ for $a = 1$, 2, and 3. Hint: Graph the functions $f(f(x))$ and $I(x) = x$ on the interval $[0, 1]$.

15.4 A period-three sequence of a map $x_{i+1} = f(x_i)$ is three different points p, q, and r for which $q = f(p)$, $r = f(q)$, and $p = f(r)$. Li and Yorke have shown that a map with a period-three sequence is chaotic. Estimate the period-three sequences of the map $f(x) = 4x(1 - x)$.